Ethyl biodiesels derived from non-edible oils within the biorefinery concept - Pilot scale production & engine emissions

S. Nitièma-Yefanova, Valérie Tschamber, Romain Richard, Sophie Thiebaud-Roux, Brice Bouyssière, Y.L. Bonzi-Coulibaly, Roher H.C. Nébié, Lucie Coniglio

Ethyl biodiesels derived from non-edible oils within the biorefinery concept – Pilot scale production & engine emissions

Svitlana Nitièma-Yefanova [a], Valérie Tschamber [b], Romain Richard [c], Sophie Thiebaud-Roux [d], Brice Bouyssiere [e], Yvonne L. Bonzi-Coulibaly [a], Roger H.C. Nébié [f], Lucie Coniglio [g, *]

[a] *Laboratoire de Chimie Analytique Environnementale et Bio-Organique, Département de Chimie, Université Ouaga I Professeur Joseph KI-ZERBO, 03 BP 7021, Ouagadougou 03, Burkina Faso*
[b] *Laboratoire Gestion des Risques et Environnement, Universite de Haute Alsace, 3B, rue Alfred Werner, 68093 Mulhouse, France*
[c] *Laboratoire de Génie Chimique, Université de Toulouse, CNRS, INPT, UPS, Toulouse, France*
[d] *Laboratoire de Chimie Agro-industrielle, Université de Toulouse, INRA, INPT, Toulouse, France*
[e] *CNRS/UNIV Pau & Pays de l'Adour, Institut des Sciences Analytiques et de Physico-Chimie pour l'Environnement et les Matériaux, UMR 5254, 64000 Pau, France*
[f] *Institut de Recherche en Sciences Appliquées et Technologies, Département Substances Naturelles, Centre National de Recherche Scientifique et Technologique, 03 BP 7047, Ouagadougou 03, Burkina Faso*
[g] *Université de Lorraine - Ecole Nationale Supérieure des Industries Chimiques de Nancy, Laboratoire Réactions et Génie des Procédés UMR CNRS 7274, 1, rue Grandville, BP 20451, 54001 Nancy Cedex, France*

Keywords:
Ethyl biodiesels
Non-edible oils
Homogeneous alkali- or acid catalysis
Dry purification
Engine emissions

A B S T R A C T

Procedures and operating conditions optimized in laboratory scale for the production of ethyl biodiesels from non-edible vegetable oils (NEVOs) were successfully transferred at pilot scale, with implementation of separation and purification stages. The three NEVOs candidates are *Balanites aegyptiaca* (BA), *Azadirachta indica* (AI), and *Jatropha curcas* (JC), converted into BAEEs, AIEEs and JCEEs respectively via homogeneous catalysis. Quality specifications of the produced biofuels were used to explain pollutant emissions and engine performance observed via a power generator. Under the same conditions, blends of petrodiesel with crude BA or JC oil (50 wt.%) were also investigated.

The selected overall methodology "feedstock-conversion-engine" led to the proposal of a sustainable alternative fuel. The candidate NEVO is BA oil to which the proposed alkali route should lead to a low cost biodiesel production process thanks to easy operating conditions, associated with a two-stage procedure (glycerol recycling) and a dry-purification method (rice husk ashes). Glycerol addition should be carried out at ambient temperature to play positively at phenomena occurring in the reacting medium (chemical kinetics, chemical equilibrium, phase equilibrium). Tests on power generator demonstrated that BAEEs led to cleaner combustion than petrodiesel, particularly for the most harmful emissions (light carbonyls and ultrafine particulate matter).

1. Introduction

The challenges in reducing the world's dependence on crude oil and the greenhouse gas effect have led to the emergence of new biofuels with improved engine performance via better fuel efficiency and reduced exhaust emissions [1]. In parallel, the sustainability of the new biofuel industries also requires to maintain a high level of biodiversity by using a variety of resources that do not compete with edible crops and conversion technologies satisfying the eco-design, eco-energy and eco-materials criteria plus flexibility in terms of geographical location [2]. Indeed, the biofuels currently marketed (the so-called first generation, 1G) are mainly produced from "edible" biomass (sugar plants and grain for bioethanol; oilseeds such as rapeseed or soybean for biodiesel) [3,4]. Additionally to a negative competition with food production, this

* Corresponding author.
E-mail addresses: snitiema@gmail.com (S. Nitièma-Yefanova), valerie.tschamber@uha.fr (V. Tschamber), romain.richard@iut-tlse3.fr (R. Richard), sophie.ThiebaudRoux@ensiacet.fr (S. Thiebaud-Roux), brice.bouyssiere@univ-pau.fr (B. Bouyssiere), yvonne.bonzi@yahoo.fr (Y.L. Bonzi-Coulibaly), neroch@hotmail.com (R.H.C. Nébié), lucie.coniglio@univ-lorraine.fr (L. Coniglio).

http://dx.doi.org/10.1016/j.renene.2017.03.058

indirect land use change (ILUC) of 1G-biofuels also leads to a negative environmental footprint, with deforestation in some areas of the globe causing a reduction in biodiversity and a displacement of pollution (CO_2 reduction through plant photosynthesis, offset by pollution-induced at soil-water during agricultural exploitation of resources (by fertilizers) and their conversion into biofuel (with generation of effluents)) [2,5].

Therefore, production of biodiesel fuel from non-edible vegetable oils (NEVOs) and bioethanol (derived from biomass residues) is an attractive alternative based on local and renewable use of agricultural resources [3,6–8]. Furthermore, this alternative would help emerging countries to access energy independence while ensuring food security and new employment sources. In addition, positive environmental balance was recognized for ethyl biodiesel (fatty acid ethyl esters, FAEEs) with lower emissions of NOx, CO, and ultrafine particles (the most harmful) than for methyl biodiesel (fatty acid methyl esters, FAMEs) [1]. Also, FAEEs have better biodegradability, higher flash point, improved cold-flow properties and oxidation stability, making them a safer fuel for storage and transportation than FAMEs [1]. However, higher emissions in carbonyls (acrolein, propanal, acetone) were observed for some FAEEs of low volatility and unsaturation level [9].

In this work, procedures and operating conditions optimized in laboratory scale for the production of FAEEs from three NEVOs locally available in Burkina Faso [10] are transferred at the pilot scale, with implementation of the separation and purification stages. In accordance with the bio-refinery concept, the selected dry purification method uses rice husk ash (RHA) derived from wastes of local production units [8]. The three NEVOs candidates, selected among biomass well adapted to arid lands and offering various upgrading pathways (drugs, cosmetics, pesticides …) valuable for development of bio-refineries [10] are *Balanites aegyptiaca* (BA, Desert date), *Azadirachta indica* (AI, Neem), and *Jatropha curcas* (JC). These were transesterified into BAEEs, AIEEs and JCEEs respectively via homogeneous catalysis identified as a simple, low-cost, and environmentally friendly route when combined with a dry purification treatment instead of water-washing [10] (supporting information-Appendix A). For the three classes of ethyl biodiesels produced, quality specifications (most relevant impurities resulting from the feedstock extraction and conversion stages, as well as key physical and thermal properties of fuels) were determined and used to explain pollutant emissions and engine performance observed via a power generator. Under the same conditions, petrodiesel was also investigated as reference fuel, as well as blends of petrodiesel with crude BA or JC oil (50 wt.%). Studies testing power generators with biofuels, particularly NEVOs either converted into ethyl biodiesels or blended with petrodiesel, are still very scarce [1,2,9]. Thus, this work will contribute to bridge some gaps in this field in favor of agricultural machinery and deployment of cogeneration in general. From this overall study "feedstock-conversion-engine", it is intended to propose a sustainable alternative fuel, particularly convenient in rural areas.

2. Materials and methods

2.1. Reagents and chemicals

Solvents (n-heptane) and other reagents (citric acid, ethanol, ethyl oleate, potassium hydroxide, sodium bicarbonate, and sulfuric acid) were of analytical grade and were purchased with the chromatographic standards (1-decanol and methyl heptadecanoate) from Merck, Acros Organics or Sigma-Aldrich. 2.4- dinitrophenylhydrazine (2,4-DNPH) was puriss. p.a. grade moistened with water and acetonitrile was CHROMASOLV® plus grade, both ≥99.0% from Sigma Aldrich. Petrodiesel (B0) was provided by Total ACS-France.

BA, AI, and JC oils were obtained by extraction (cold pressing and filtration) of the seed kernels [11]. Characterization of the three NEVOs in terms of fatty acid composition and key properties as feedstocks to ethanolysis were conducted in previous works and are here summed up respectively in Tables 1 and 2 [10,12].

Regarding the RHA production, rice husks from local production units (Burkina Faso) were finely ground, carbonized in a muffle furnace (MF4 Hermann Moritz Regulateur 2068, France) at 500 °C for 8 h, and then cooled to room temperature in desiccators for 8 h minimum [8]. The incineration process was conducted with a mean yield of 18 ± 1 wt.% (percent ratio of the mass of recovered ashes to the mass of initial rice husk). Incomplete carbonization of the rice husk led to a heterogeneous mixture consisting of two main classes of ashes, RHA-LG (for the light-grey ashes) and RHA-GB (for the grey-black ashes), with respective mass fractions of 43 and 57 wt.%. Furthermore, in a previous work [8], scanning electron microscopy (SEM) coupled with microanalysis by energy dispersive X-ray spectroscopy (EDS) had revealed that both classes of ashes looking similar to corn cobs were rich in silicon (in the outer epidermis) and in potassium (in the inner part and cross-sections showing large size pores). Nevertheless, containing activated carbon (on the basis of the ash color and results obtained in the literature [18]) with a micro-/macroporous structure of high specific area (202 ± 2 m^2/g determined by the Brunauer–Emmett–Teller (BET) method [8]), the RHA-GB had shown higher performance as purifying agent [8] and was then selected in this work.

2.2. Biodiesel production

All experiments and analyses related to AI and JC oils were conducted in duplicate, and from each set of duplicates, an average value was then calculated to yield to the given data. By contrast, BA oil ethanolysis was conducted in triplicate in order to evaluate the standard deviations on conversion and BAEE mass fractions; results are then given in terms of average ± standard deviation. Furthermore, overall material balance (together with yield in FAEEs) was evaluated to check the validity of each experiment.

2.2.1. Reaction & separation

With respect to the FFA content of the departure lipid feedstocks (Table 2), the BAEEs and AIEEs were obtained *via* alkali catalysis (potassium hydroxide, KOH) and the JCEEs via acid catalysis (sulfuric acid, H_2SO_4). A two-stage procedure via intermediate addition of glycerol allowed the enhancement of ethanolysis yields. The operating conditions optimized at the laboratory scale [10] and transferred at the pilot scale are summarized in Table 3. Only the stirring parameters (speed and duration) of the acid catalysis procedure were changed during the pilot scaling to overcome the mass transfer limitation occurring at the start of the reaction, until formation of sufficient amount of esters in the medium. Regarding the main features of the procedures transferred at the pilot scale, alkali (acid) catalysis was operated at 35 °C (78 °C), with an alcohol to oil molar ratio equal to 8:1 (30:1), anhydrous (95 wt.% ethanol, 5 wt.% water) ethanol as alcohol, a catalyst concentration of 1 wt.% (5 wt.%) based on the initial mass of oil, a reaction time of 50 min (26 h) while the addition of glycerol marking the start of the second-stage was carried out after 30 min (8 h) of reaction. A scaling factor of 25 (16) was applied for the alkali (acid) catalysis. The pilot scale equipment (Thermo Fisher Scientific, France) is shown in Fig. 1. A 4 L double-jacketed reactor made of durable borosilicate glass is temperature controlled via a PT100 PTFE probe (± 0.15 °C) connected to a CRYOPOLYSTAT (−35 to 200 °C). Efficient stirring is insured via PTFE baffles and impeller blades mounted via a central driveshaft on an IKA-Eurostar Power Control-Visc stirrer

(50–1200 rpm). A five-necked lid allows for completing the equipment with a condenser (both made of durable borosilicate glass) and a sampling syringe connected to a long needle. At the bottom of the reactor elliptical in shape, a valve without dead volume permits the racking of glycerol, and then of FAEEs, after phase separation. Further details can be found in Ref. [19]. Similarly to the laboratory scale, ethanolysis was monitored by gas-chromatography analysis coupled with a flame ionization detector (GC-FID), at a sampling frequency dictated by the reaction conditions [10]. Information specific to the GC-FID analysis with preliminary neutralization of samples are given in Table A1 (Appendix) while details related to the FAEE identification and quantification are provided in the work developed at the laboratory scale [10] (main text and supporting information-Appendix B).

After carrying out the phase separation within the reactor, and then withdrawing first the glycerol rich phase and then the FAEE rich phase via the bottom racking, both phases were weighed. Residual ethanol in each phase was then evaporated (at 70 °C and 180 mbar, for 1.5 h) helping thus to separate and quantify the key components of the reaction mixture (FAEEs, glycerol and ethanol) [20], and estimate their distribution between each phase.

2.2.2. Purification

The produced RHA-GB (section 2.1) was used as natural adsorbent to purify the three classes of FAEEs from NEVOs (BAEEs, AIEEs and JCEEs). With reference to results obtained for various dry purification procedures [8], the "*flash method*" (one stage treatment carried out with 4 wt.% of RHA-GB in the unpurified FAEE sample, at 20 °C under stirring for 5 min followed by vacuum filtration) was selected here as a satisfactory trade-off between efficiency and energy cost. Details of the equipment and operating conditions used to characterize the three classes of FAEEs before and after dry purification on RHA-GB are summarized in Table A1 (Appendix). Characterization was carried out by quantifying molecular species different in size and shape such as triacylglycerides (TG), diacylglycerides (DG), monoacylglycerides (MG), free glycerin, water and FAEEs, but also potassium and heavy metals (resulting from the catalyst used and the oil extraction stage).

2.3. Fuel properties of the produced biodiesels

Physical properties of the three classes of biodiesel produced (BAEEs, AIEEs, and JCEEs) were experimentally determined according to ASTM standards (D-4052-96 for the density at 15 and 25 °C; D-445 for the kinematic viscosity at 37.8 °C; D97-93 for the cloud point; D2500-91 for the pour point). By contrast, key thermal properties such as lower heating value (*LHV*) and brake specific energy consumption (*BSEC*) were calculated from measurements of the higher heating value (*HHV*) and brake specific fuel consumption (*BSFC*) respectively. The *HHV* of each fuel was experimentally determined via an IKA-C200 calorimeter (Germany) while the *BSFC* was measured during analysis of emissions and engine performance (section 2.4). The equations used for calculating the *LHV* and *BSEC* are given below.

$$LHV = HHV - L_C \cdot m_w \tag{1a}$$

where $L_C = 2486\ \mathrm{kJ \cdot kg^{-1}}$ is the latent heat of condensation of water at 273 K and atmospheric pressure, and m_w (kg) is the mass of water in 1 kg of fuel estimated by:

$$m_w = (\overline{x}_w + 9\ \overline{x}_H)/100 \tag{1b}$$

with the water and hydrogen contents of the fuel, $\overline{x}_w$ and $\overline{x}_H$ (wt.%), determined from analysis ($\overline{x}_w$: Karl Fischer titration; $\overline{x}_H$: estimation given the FAEE composition of the fuel via GC-FID, Table A1).

$$BSEC = (BSFC \cdot LHV)/1000 \tag{2}$$

with *BSEC* in $\mathrm{MJ \cdot kWh^{-1}}$, *BSFC* in $\mathrm{kg \cdot kWh^{-1}}$ and *LHV* in $\mathrm{kJ \cdot kg^{-1}}$.

2.4. Emission analysis: equipment & protocol

Combustion of the produced biodiesels (BAEEs, AIEEs, JCEEs) along with two of the parent crude NEVOs (BA and JC) blended with petrodiesel (B0) was performed in a diesel generator. Indeed, within a farm context, it is relevant to consider the direct use of crude NEVOs or their FAEEs as engine fuel. However, using neat crude NEVOs as fuel led to engine breakdowns. Hence, a mass ratio of 50:50 was used for the blends designated by [BA:B0] and [JC:B0]. All results were compared with those obtained from the combustion of petrodiesel B0 taken as reference fuel.

A detailed description of the whole experimental set-up can be found in Refs. [9,21], thus only the main features are given here. The test rig used consists of the diesel generator, a fuel tank and an exhaust pipe equipped with sampling probes linked to different analyzers allowing the analysis of the exhaust composition, in term of gaseous and particulate pollutants. The diesel generator provided by Yanmar (France) is composed of a one cylinder engine with a displacement volume of 0.296 L. The engine power is equal to 4780 W with a maximum electrical power of 3400 W. A generator load of 3000 W was tested in this study using a bench of 500 W lamps. The consumption of the fuel was evaluated using a gravimetric method. Temperature of the exhaust, at the place of the probes, was recorded and the gas flow was determined using a venture system. In our conditions, the gas temperature was ranging from 308 to 312 °C. Relevant details on the analyzers are given in Table A1 (Appendix).

Gaseous emissions CO, CO_2, NO, NO_2, O_2 and total hydrocarbons (HC) in the exhaust were analyzed with a HORIBA MEXA 7100D (expressed in % or ppm). It was preceded by a heated back-flushing filter (HBF) to remove particulate matter and avoid water condensation. The HC emissions were quantified by FID analyzer, CO and CO_2 with a non-dispersive infrared (NDIR) analyzer, and O_2 with a magneto pneumatic analyzer. A chemiluminescence analyzer was

Table 1
Composition in terms of fatty acids (molar fractions %) of the three NEVOs investigated: *Balanites aegyptiaca* (BA), *Azadirachta indica* (AI), and *Jatropha curcas* (JC) [12]

Fatty acids - Formulae *(name)*	Burkina Faso NEVO		
	BA	AI	JC
C10:0 *(Capric acid)*	0.05	0.05	0.05
C12:0 *(Lauric acid)*	0.02	0.02	0.01
C13:0 *(Tridecanoic acid)*	0.02	0.02	0.03
C14:0 *(Myristic acid)*	0.06	0.05	0.06
C16:0 *(Palmitic acid)*	**13.79**	**17.65**	**15.56**
C16:1c9 *(Palmitoleic acid)*	0.14	0.11	0.92
C17:0 *(Heptadecanoic acid)*	0.11	0.13	0.08
C18:0 *(Stearic acid)*	**11.07**	**17.46**	**7.34**
C18:1t9 *(Elaidic acid)*	0	0.21	0
C18:1c9 *(Oleic acid)*	**28.25**	**46.84**	**42.53**
C18:1c11 *(cis-Vaccenic acid)*	0.72	0.52	1.23
C18:2c9c12 *(Linoleic acid)*	**45.32**	**14.90**	**31.84**
C18:3c9c12c15 *(Linolenic acid)*	0.06	0.44	0.16
C20:0 *(Arachidic acid)*	0.33	1.55	0.19
C22:5c7c10c13c16c19 (*Docosapentaenoic acid*)	0.06	0.05	0
Total	100.00	100.00	100.00
Saturated species	25.45	36.93	23.32
Monounsaturated species	29.11	47.68	44.68
Polyunsaturated species	45.44	15.39	32.00

Major components are indicated in bold.

Table 2
Key properties of the three NEVOs selected as feedstocks for ethanolysis (*Balanites aegyptiaca* (BA), *Azadirachta indica* (AI), and *Jatropha curcas* (JC)) [10].

Key properties	Burkina Faso NEVO		
	BA	AI	JC
Average molecular weight[a]	857	829	849
Water content (wt.%)[b]	0.06	0.07	0.08
Acid value (mg KOH/g)[c]	0.46	4.54	25.36
Acidity (%)[c]	0.23	2.29	12.74

[a] Calculated from the oil molar composition in terms of fatty acids.
[b] Determined by Karl-Fischer titration.
[c] Determined by following the standard EN-14104 [13].

used to quantify NO and NO_2. The chemiluminescence analyzer separately measured NOx and NO, and then NO_2 concentration was obtained by subtracting the NO contribution from the NOx measurements (Table A1, Appendix).

Fine (PM10 and PM2.5) and ultrafine (PM1 and PM0.1) particle concentration and distributions were analyzed using on line particle sizing technique. The aerosol measurement system includes a Fine Particle Sampler (FPS-4000) for diluting and conditioning aerosol, as well as an Electrical Low Pressure Impactor (ELPI) to measure airborne real time particle size distribution and concentration in the size range of 30 nm to 10 μm (Table A1, Appendix). The aerosol sample was extracted from the exhaust by using a stainless steel heated line (120 °C). The sample is subsequently diluted in two stages. The primary dilution air is heated to 120 °C to prevent nucleation and condensation. The second dilution stage occurs in an ejector-type diluter. The ejector diluter acts as a pump which draws the sample from the primary dilution stage and dilutes it further. The secondary diluted gas exiting the ejector diluter is always at ambient pressure and temperature. Dilution, temperatures and pressures are measured in real-time by a control unit enabling dilution ratio calculation second-by-second, which directly takes into account the changes in raw sample properties. In this study diluting ratios of 10:1 to 15:1 were used. The diluted sample is then introduced into the cascade impactor system (ELPI) that separates the particle matter following aerodynamic equivalent cut-off diameter at 50% efficiency in twelve particle size fractions ranging from 30 nm to 10 μm.

In order to analyze formaldehyde, acetaldehyde, acrolein, acetone, propanal, butanal and benzaldehyde, exhaust gas was pumped and came firstly through a filter in order to eliminate soot

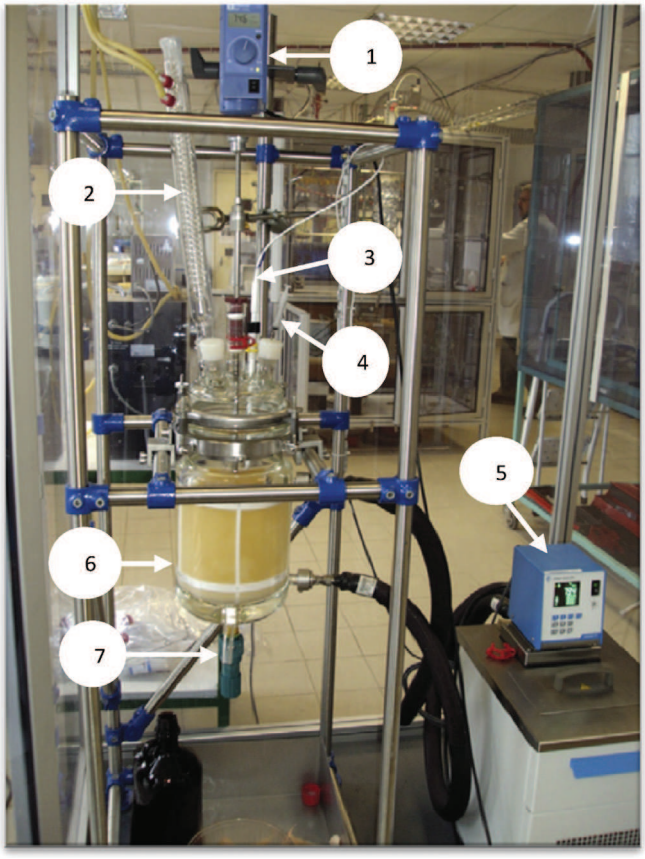

Fig. 1. Experimental pilot scale device for ethanolysis of NEVOs. Legend: (1) IKA-Eurostar Power Control-Visc stirrer (50–1200 rpm); (2) condenser; (3) PT100 PTFE probe (± 0.15 °C); (4) sampling syringe; (5) CRYOPOLYSTAT (−35 to 200 °C); (6) 4 L double-jacketed reactor elliptical in shape with PTFE baffles; (7) racking bottom valve without dead volume; (2) and (6) are made of durable borosilicate glass (Thermo Fischer Scientific, France) [19].

from the effluent then through three impingers filled with 150 mL of a 2,4-DNPH solution at 1.23 g L^{-1} and put in sequence. Sampling was performed for 1 h at 1 L min^{-1}. The samples were then analyzed with a High Performance Liquid Chromatography (HPLC) coupled with a UV detector system (Table A1, Appendix). Acetone, acrolein and propanal were quantified together due to the

Table 3
Pilot scale operating conditions for ethanolysis of the three NEVOs investigated.

NEVO	BA and AI	JC
Nature of the catalyst	KOH	H_2SO_4
First stage		
Reaction temperature/°C	35	78
Ethanol characteristics	Anhydrous	Hydrated (95 wt.%)
Ethanol to oil molar ratio	8:1	30:1
Catalyst concentration (wt.%)[a]	$1 + x$	5
Stirring (rpm)	250	750, for the first 4 h then, 250 until the end of the first stage[b]
Second stage		
Reaction temperature/°C	35	20 °C at ambient air for 18 h
Addition of fresh glycerol at the specified reaction time[c]	30 min	8 h
Stirring (250 rpm)	Yes (5 min)	Yes (5 min)
Total duration of the reaction	50 min	26 h

[a] Based on the initial mass of oil, with x calculated given the NEVO acid value.
[b] Only this parameter was changed from the procedure optimized at the laboratory scale (initially equal to 250 rpm for all the first stage period) in order to overcome the mass transfer limitation until a sufficient amount of esters is formed to lead to a homogeneous mixture (i.e. 4 h of reaction at the pilot scale).
[c] 25 wt.% based on the initial weight of oil.

difficulties in resolving the chromatographic peaks using an isocratic elution.

3. Results and discussion

3.1. Pilot scale biodiesel production

The fundamental aspects underpinning the following discussion are available in earlier published works developed at the laboratory scale, both for the reaction & separation stages [10] (supporting information-Appendix A) and the dry-purification stage [8]. These fundamental aspects focus on the main physicochemical features of ethanolysis (NEVO conversion to biodiesel via transesterification methods; reduced mass transfer limitation; coupling of chemical kinetics, phase equilibria and chemical equilibrium; key parameters of the ethanolysis process and best compromise) and on the relationship between the structure and composition of various natural materials versus their adsorbent efficiency. Consequently, results will be discussed in the following on the basis of conclusive justifications derived from these fundamental aspects, by focusing on the transfer from the laboratory scale to the pilot scale.

3.1.1. Reaction & separation

Evolutions of FAEE contents vs. time obtained during ethanolysis of the three NEVOs are depicted in Figs. 2–4. As it can be observed in Fig. 2, the procedure and operating conditions optimized in laboratory scale for the alkali-catalyzed ethanolysis of BA oil [10] have been successfully transferred at the pilot scale, with almost constant BAEE content of 92 wt.%. Furthermore, the whole results related to the pilot scale BA oil ethanolysis were obtained with satisfactory repeatability. Regarding the alkali-catalyzed ethanolysis of AI oil (Fig. 3), similar conclusions can be drawn, with even a slight enhancement of the ester content to reach 91 wt.% after pilot scale transfer. Nevertheless, a better fit of the stirring speed in relation to the larger reactor volume should enhance both yields in BAEEs and AIEEs. On the other hand, the other key parameters of ethanolysis (catalyst, alcohol to oil molar ratio, temperature) being appropriately balanced maintain the procedure efficient to guarantee satisfactory yields in FAEEs. Thus, the amount of catalyst (around 1 wt.% KOH) accelerates enough ethanolysis without promoting however formation of stable

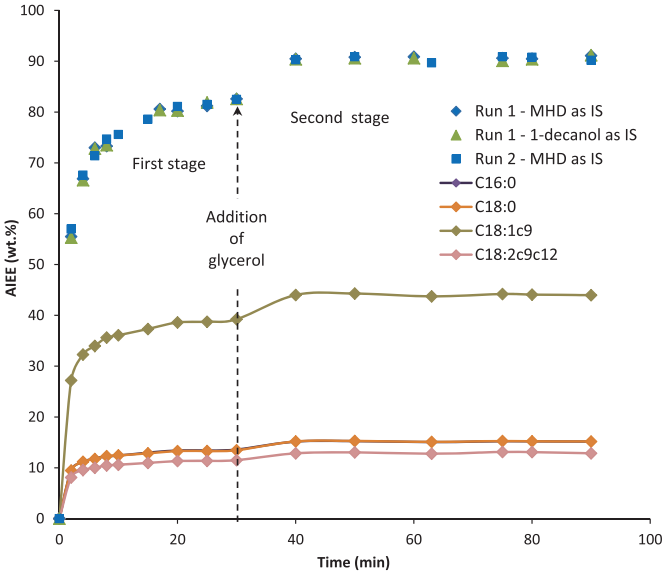

Fig. 3. AI oil ethanolysis at the pilot scale (C16:0 and C18:0 profiles are superimposed on each other, in accordance with AI oil composition in terms of fatty acids given by Table 1).

emulsions. Also, the selected ethanol to oil molar ratio (8:1) is high enough compared to stoichiometry (3:1) for limiting reversibility of ethanolysis while improving (together with stirring) reactants' miscibility and thus mass transfer, but is not too high for making inefficient the two-stage procedure based on intermediary addition of glycerol. This one generating liquid-liquid demixing of the ethanolysis mixture (and thus, glycerol removal from the reaction phase with further shifting of the ethanolysis chemical equilibrium towards FAEE production), is also favored by the low temperature selected (35 °C, apparently not too low for inhibiting the mass transfer).

By contrast, results related to the scale up of the acid-catalyzed ethanolysis of JC oil (Fig. 4) were less satisfactory, with a significant decrease of the JCEE contents from 89 to 84 wt.% during transfer

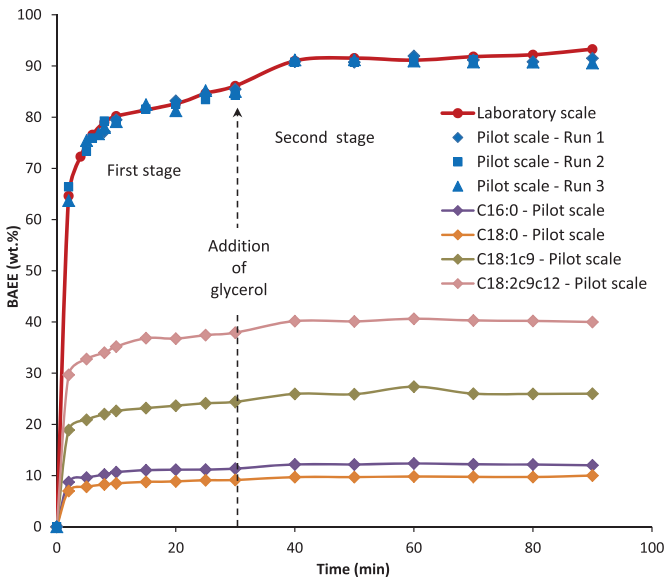

Fig. 2. BA oil ethanolysis from the laboratory to the pilot scale (scale factor: 25).

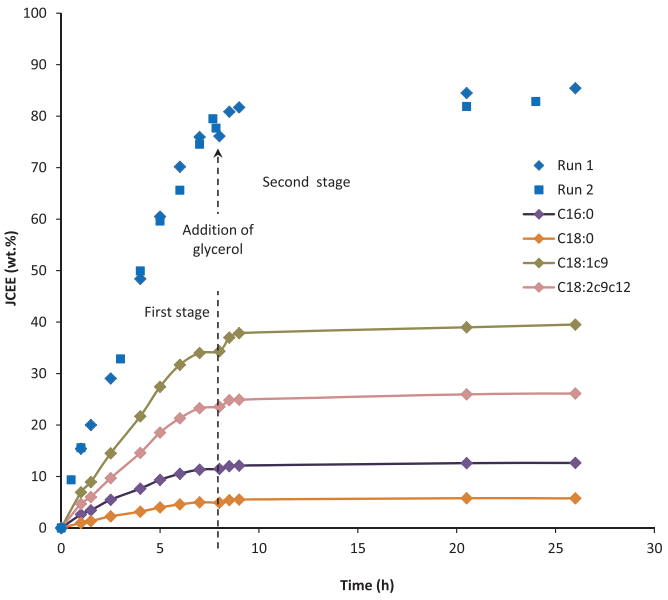

Fig. 4. JC oil ethanolysis at the pilot scale.

from the laboratory scale to the pilot scale. Yet, Fig. 4 shows no changes in evolution of JCEE content vs. time (no mass transfer limitation at the early stage of ethanolysis and increase of the JCEE content induced by addition of fresh glycerol), except for the plateau depicting the chemical equilibrium that moved to a lower level. Hence, alcohol to oil molar ratio and temperature of reaction seem adequate, but other operating conditions need to be optimized further. More specifically, stirring efficiency and duration expected for the glycerol decantation (due to inertia of the system for cooling) should be revised. Also, an additional stage for partial evaporation of ethanol before addition of glycerol should be introduced in the procedure to promote the reaction mixture phase separation.

Indeed, as highlighted by Table A2 (see Appendix), distributions of ethanol, glycerol and FAEEs between the two phases obtained after separation of the final reaction mixture have very different behaviors depending of the type of catalysis (alkali or acid). More precisely, it was observed that the ester-rich phase obtained via acid catalysis contained about 11% less ethanol but 2% more glycerol in mass than that obtained via alkali catalysis. Consequently moving from one phase to the other, the proportion of ethanol in the glycerol-rich phase was 11 wt.% higher (2 wt.% lower regarding glycerol proportion) when ethanolysis was conducted under acid catalysis. Even more challenging, the glycerol-rich phase in the same conditions contained a significant fraction of esters (16 wt.%), unlike the alkali-catalysis. Admittedly, the water content of the alcohol used for JC oil ethanolysis (hydrated ethanol 95 wt.%) promotes the solubility of ethanol and thus also FAEEs in the glycerol-rich phase (water affinity for glycerol being the driving force); however, the high values of both temperature and alcohol to oil molar ratio of the acid catalysis should be further impacting.

From the foregoing, it is clear that conducting ethanolysis under high temperature, with also a large excess of ethanol, promotes significantly the miscibility of the two liquid phases. This phenomena limits the chemical equilibrium shifting towards formation of products of very low-miscibility (FAEEs and glycerol) and thus makes even more challenging the separation stage, the whole leading to lower yields in esters and in glycerol. A more efficient removal of ethanol should be required to enhance the phase separation, and thus, recover properly the esters moved to the glycerol-rich phase under acid catalysis conditions (particularly when hydrated ethanol is used) [10].

As a result, satisfactory errors in overall material balances (OMBs) were obtained for experiments related to the alkali-catalyzed ethanolysis of BA and AI oils (1.3 and 1.5 wt.% respectively), while the error has doubled for the acid-catalyzed ethanolysis of JC oil (2.7 wt.%) (Table A3, see Appendix). Consumed ethanol to oil molar ratios estimated from OMB data (i.e. 3.6:1, 3.4:1, and 6.4:1 for respectively BA, AI, and JC oil, Table A3) being larger than the stoichiometric molar ratio (3:1 alcohol to oil) confirm these experiment uncertainties. These can be explained by an incomplete recovery of the excess ethanol, particularly for the JC oil acid-catalyzed ethanolysis. Indeed, in that case, ethanol recovery from the glycerol-rich phase was more difficult than in alkali-catalysis because of the enhanced mutual solubility of glycerol and hydrated ethanol at high temperatures (as highlighted previously, Table A2). Moreover, condenser was efficient during reaction to avoid any ethanol loss. Regarding yields in FAEEs, values superior to 100 wt.% were reached for BA and JC oils (102 and 105 wt.% respectively). In addition to incomplete recovery of ethanol and thus glycerol in the ester-rich phase, this is also due to the reaction stoichiometry (3 mol of FAEEs for 1 mol of TG) leading to a higher mass of FAEEs for a lower mass of TGs (e.g.: 931 g of ethyl oleate for 885 g of triolein). By contrast, the lower yield reached for AI oil ethanolysis (93 wt.%) results from a more tedious phase separation with material loss due to the contents in saturated glycerides and FFAs of the departure oil (Tables 1 and 2). Indeed, these induce respectively a higher viscosity of the medium (with mass transfer limitation) and formation of soaps (with emulsions) [10] (supporting information-Appendix A).

Finally, pure glycerol was added to the reaction mixture. However, recycling crude glycerol obtained as by-product from biodiesel production process would be the suitable option for industrial purposes. Moreover, glycerol would be rich in catalyst, and thus may enhance even more oil conversion. Furthermore, Figs. 2–4 confirm that the ethanolysis kinetics is established by the major fatty acid of the departure feedstock, i.e. linoleic acid (C18:2c9c12) for BA oil and oleic acid (C18:1c9) for AI and JC oils. Also, as illustrated by Fig. 3, both tested internal standards yield very close estimations of the FAEE contents, confirming that 1-decanol performs as well as methyl heptadecanoate (MHD) [10] recommended by the European Standard EN-14103 [22].

3.1.2. Dry purification

The dry purification yields (defined as Y_i (wt.%) $= (m_i/m_0) \times 100$ with m_i and m_0 the mass of sample before and after treatment respectively) were 95 ± 1 wt.% for the three FAEE products (BAEEs, AIEEs, and JCEEs). Results of their characterization before and after dry purification, along with of treatment efficiency, are shown in Table 4 for molecular species and Table 5 for chemical elements. Furthermore, it is important to mention that GC-FID analyses revealed no residual TG in the unpurified FAEE products, which

Table 4
Characterization of FAEE products with regards to their molecular components before and after dry purification.[a] Efficiency of the dry purification method for the focused contaminants is also given in brackets.[b]

Treatment stage of the FAEE product	Esters (wt.%)	Free glycerin (wt.%)	MG (wt.%)	DG (wt.%)	Total glycerin (wt.%)	Water (mg/kg)
Balanites aegyptiaca fatty acid ethyl esters (BAEEs)						
Unpurified BAEEs of departure	91.51	0.13	3.14	0.48	1.00	466
BAEEs after dry-purification	92.13	0.09 *(-31)*	2.40 *(-24)*	0.45 *(-6)*	0.77 *(-23)*	414 *(-11)*
Azadirachta indica fatty acid ethyl esters (AIEEs)						
Unpurified AIEEs of departure	90.61	0.20	2.75	0.56	0.98	318
AIEEs after dry-purification	90.36	0.08 *(-60)*	2.22 *(-19)*	0.40 *(-29)*	0.70 *(-29)*	303 *(-5)*
Jatropha curcas fatty acid ethyl esters (JCEEs)						
Unpurified JCEEs of departure	84.30	0.15	2.60	0.91	0.95	875
JCEEs after dry-purification	83.80	0.13 *(-13)*	3.42 *(+32)*	0.93 *(+2)*	1.14 *(+20)*	918 *(+5)*
Specifications of EN-14214[c]	**96.5**	**0.02**	**0.80**	**0.20**	**0.25**	**500**

Specifications of EN-14214 are indicated in bold.
[a] Standard deviation on esters, free glycerin, MG, DG, and total glycerin (wt.%): 0.05.
[b] Method efficiency assessed as a function of removal percentage of each contaminant (η_c) calculated by $\eta_c = 100 \times (x_f - x_0)/x_0$, where x_0 and x_f are the contents of each contaminant before and after treatment.
[c] All indications are limits, except for the ester content giving the maximum value.

Table 5
Characterization of the inorganic composition of FAEE products before and after dry purification.[a] Efficiency of the dry purification method for the focused contaminants is also given in brackets.[b]

Treatment stage of the FAEE product	Chemical element contents (mg/kg)						
	Si	K	S	Ca	Mg	Fe	P
Balanites aegyptiaca fatty acid ethyl esters (BAEEs)							
Unpurified BAEEs of departure	0.63	35.0	6.4	0.72	<0.2	<0.2	<0.2
BAEEs after dry-purification	0.50 *(-21)*	9.4 *(-73)*	1.8 *(-72)*	0.42 *(-42)*	<0.2	<0.2	<0.2
Azadirachta indica fatty acid ethyl esters (AIEEs)							
Unpurified AIEEs of departure	4.23	34.6	370	0.49	0.32	0.20	<0.2
AIEEs after dry-purification	4.00 *(-5)*	12.8 *(-63)*	360 *(-3)*	0.42 *(-12)*	<0.2 *(-38)*	<0.2	<0.2
Jatropha curcas fatty acid ethyl esters (JCEEs)							
Unpurified JCEEs of departure	8.96	2.6	7.9	<0.2	<0.2	<0.2	<0.2
JCEEs after dry-purification	11.92 *(+33)*	8.4 *(+223)*	10.3 *(+30)*	0.21 *(+5)*	<0.2	<0.2	<0.2
Specifications of EN-14214[c]	-[d]	**5**[e]	**10**	**5**[f]	**5**[f]	-[d]	**10**

Specifications of EN-14214 are indicated in bold.
[a] Detection limits (mg/kg) of the analytical method used (ICP-AES): 0.2 for Ca, Mg, Fe and P; 0.4 for Si; 1 for K and S; Maximum standard deviation (mg/kg): 0.01 for Fe; 0.03 for Mg and Ca; 0.06 for Si; 0.3 for K and S (with the exception of AIEEs with sulfur high contents: 1).
[b] Treatment efficiency assessed as a function of removal percentage of each contaminant calculated by $\eta_c = 100 \times (x_f - x_0)/x_0$, where η_c is the efficiency of the dry purification treatment, x_0 and x_f are the contents of each contaminant before and after treatment, respectively; for a contaminant content below or equal to the observed ICP-AES detection limit, this latter value was used to evaluate the treatment efficiency.
[c] All indications are limits.
[d] No specification exists regarding this species.
[e] For (Na + K).
[f] For (Ca + Mg).

moreover contained relatively high ester contents (around 92, 91, and 84 wt.% for the BAEEs, AIEEs, and JCEEs, respectively). Moreover, the observed Fe, Mg, and P contents in the initial FAEE products were mostly below detection limits of the analytical method used. These features of the initial material to be purified should also be considered as factors impacting the following observations and discussion.

The results as a whole clearly demonstrate effectiveness of dry purification treatment for the FAEE products obtained by alkali-catalyzed ethanolysis. Furthermore, this performance is observed for contaminants showing differences in shape and size, thanks to the micro-/macro-porous structure of the adsorbent RHA-GB highlighted previously by SEM and BET analyses [8] (section 2.1). Indeed, the impurity levels of BAEEs and AIEEs, such as organic materials (residual glycerides and free glycerin) or inorganic materials (water and metals) were significantly reduced (Tables 4 and 5), although the EN-14214 Standard requirements are not fulfilled for most contaminants. By contrast, poor performance is observed for the dry purification of JCEEs obtained by acid-catalyzed ethanolysis, irrespective of the fact that the JCEEs were processed in a borosilicate glass reactor for a much longer reaction time (26 h) than the BAEEs and AIEEs (50 min) promoting contamination by Si and thus a high initial level of this element in the JCEEs. Actually in that case, with the exception of free glycerin, contents in all other contaminants increased significantly after treatment over RHA-GB. More specifically, a supplementary production of MG (Table 4) along with increase in K and Si contents (Table 5) in JCEEs post dry treatment suggest (*i*) the occurrence of chemical reactions inside the adsorbent macropores activated by residual H_2SO_4 and (*ii*) the release by the ashes of part of their chemical elements in the permeant. Indeed, as mentioned in section 2.1, SEM/EDS analyses of RHA-GB highlighted the occurrence of high contents in K and Si. Furthermore, in a previous work [8], comparison of the SEM images of a sample of virgin RHA-GB with a sample of used RHA-GB recovered after a purifying treatment of FAEEs produced via acid-catalysis (followed with a supplemental incineration stage) revealed a district change in the morphology of the ashes with the appearance of larger size pores in the cross-sections On the other hand, this phenomenon was not observed with FAEEs produced via alkali-catalysis [8]. Such a macroporous structure promotes

Table 6
Key physical and thermal properties as fuels for the three classes of ethyl biodiesels produced from NEVO, for the neat NEVO and their blends with petrodiesel (NEVO to petrodiesel mass ratio 50:50).[a]

Property	Units	BAEEs	AIEEs	JCEEs	BA	AI	JC	Petrodiesel
Density (15 °C)	kg/m^3	877	875	877	920	919	918	795[b]
Density (25 °C)	Kg/m^3	870	868	870	913	912	911	ND
Kinematic viscosity (37.8 °C)	cSt (mm^2/s)	4.87	4.90	4.69	38.05	45.75	37.72	2.6[c]
Cloud point	°C	3	ND	3	1	8	1	−20[d]
Pour point	°C	ND	6	ND	0	6	0	−35[d]
HHV	MJ/kg	38.695	39.246	38.573	38.701	ND	38.735	47.320
LHV	MJ/kg	35.982	36.484	35.846	35.988	ND	36.008	44.800[d]
Water content	(wt.%)	0.041	0.030	0.092	0.06	0.07	0.08	0.003
Hydrogen content	(wt.%)	12.1	12.3	12.2	12.1	12.3	12.2	13.5
Fuel consumption	(kg/h)	0.841	0.844	0.868	0.835[e]	ND	0.823[e]	0.725
BSFC	kg/kWh	0.336	0.338	0.347	0.334[e]	ND	0.329[e]	0.290
BSEC	MJ/kWh	12.1	12.3	12.4	12.0[e]	ND	11.8[e]	12.9

[a] All properties denoted by ND were not determined.
[b] Determined at 20 °C.
[c] Determined at 40 °C.
[d] Average value [27].
[e] NEVO & petrodiesel blends (mass ratio 50:50).

diffusion of species and their adsorption in this region. Thus, RHA-GB seems to act as the support of the residual acid catalyst used for the JC oil ethanolysis and contributes to restart the acid activity through heterogeneous catalysis reactions during the dry-purification treatment of the JCEEs. These points corroborate that dry purification over RHA-GB should not be used for biodiesels obtained *via* acid catalysis [8]. In such case, liquid-liquid extraction with crude glycerol resulting from biodiesel production via alkali catalysis [23] might be a better option.

Also, the very high sulfur concentration in the purified AIEEs (35 times higher than the limit imposed by EN-14214 [24], Table 5) is due to the presence of volatile organosulfur components in the initial lipid resource [25,26]. Thereby, it is not surprising that treatment over RHA-GB did not succeed to bring sulfur level in the AIEEs below the EN 14214 Standard requirements.

3.2. Biofuel key physical and thermal properties

Key physical and thermal properties of ethyl biodiesels produced from the three selected NEVOs, together with the crude NEVO and their blends with petrodiesel (mass ratio 50:50), are gathered in Table 6. As it can be observed, the three biodiesels BAEEs, AIEEs, JCEEs, and petrodiesel show very similar physical properties, highlighting why biodiesels in general, including the produced ones, are strong fuel candidates for diesel engines.

Cloud points for BAEEs and JCEEs are 2 °C higher than the one of the parent crude NEVO, whereas the pour points of AIEEs and crude AI oil are analogous. Furthermore, all ethyl biodiesels and parent crude NEVOs exhibit similar *LHV* (lower heating values) which are however lower than for petrodiesel fuel. The lower *LHV* observed for all classes of produced biodiesels together with their parent NEVO justify a higher fuel consumption during their combustion in diesel engine. Nevertheless, this drawback is counterbalanced by a higher *BSEC* value observed for the petrodiesel fuel compared with other renewable fuels.

3.3. Biofuel emission characteristics

This section deals with the emission characteristics of all biofuels for which the key physical and thermal properties were previously determined, that is the produced ethyl biodiesels (BAEEs, AIEEs, JCEEs), and two of the parent crude NEVOs (BA and JC) blended with petrodiesel B0 (mass ratio of 50:50) designated by [BA:B0] and [JC:B0], with B0 taken as reference fuel for comparison.

3.3.1. Gaseous pollutant and CO_2 emissions

Gaseous emissions of HC, CO, NOx, and CO_2 from combustion of the whole tested biofuels are listed in Table A4 (Appendix) and depicted in terms of percent variations compared with petrodiesel B0 in Fig. 5.

As it can be observed, all biofuels (BAEEs, AIEEs, JCEEs, but also [BA:B0] and [JC:B0] blends) produced higher levels of CO_2 emissions than neat B0 fuel. This result which is generally observed for most lipid-derived biofuels is attributed to the presence of the ester group in their molecular structures, involving thus a higher oxygen content that helps to obtain a more complete and cleaner combustion [1,2,28]. Therefore, in accordance with literature related to the same NEVO feedstocks [28–31], decrease in CO and HC emissions were simultaneously observed for BAEEs and AIEEs compared with B0 (respectively 3 and 7% CO emission reduction; 12 and 3% for HC emissions). By contrast, JCEE biodiesel, as well as [BA:B0] and [JC:B0] blends, exhibit quite higher levels of CO and HC emissions compared to B0 (respectively 16, 29 and 33% for CO; 5, 12 and 17% for the HC). Regarding JCEE biodiesel, these results may be attributed to an inferior purity grade (ester content of 83.8 wt.%) with

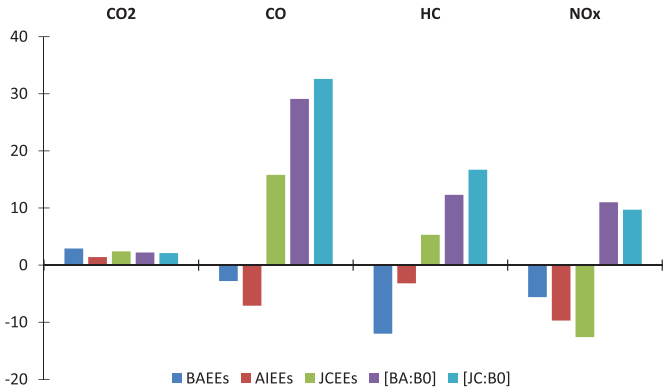

Fig. 5. Percent variations of gaseous emissions from combustion of the produced ethyl biodiesels (BAEEs, AIEEs, JCEEs) and parent NEVOs (BA and JC) blended with petrodiesel B0 (mass ratio 50:50) compared with B0.

thus too high levels of residual glycerides of high boiling points, leading to unburnt hydrocarbons in the combustion chamber. Besides, the analogous tendency observed for the CO and HC emissions from combustion of [NEVO:B0] blends rich in glycerides (main components of the NEVO) confirms this assumption. In addition, an increase in total glyceride content induces higher viscosity of the fuel, which impacts significantly CO and HC emissions by increasing even more their levels. Indeed, high viscosity leads to a more difficult atomization/vaporization of the fuel compared to petrodiesel; this creates locally fuel-rich areas inside the combustion chamber, leading to large CO and HC production because of incomplete combustion by air default. In addition, viscosity and density being directly linked to cetane number, which are all correlated to species molecular structure [1,32,33], CO and HC exhaust emissions should be more governed by the physical properties and chemical groups of the fuel than by its oxygen content. This is confirmed by the much higher CO and HC emissions produced by the [NEVO:B0] blends, exhibiting a much higher viscosity compared to B0.

Regarding NOx emissions, all ethyl biodiesels resulted in significant decreases (6, 10 and 13% for BAEEs, AIEEs, and JCEEs respectively), whereas [NEVO:B0] blends led to higher levels (12 and 16% when using respectively BA or JC as NEVO). Results observed in this work for ethyl biodiesels confirm the controversy found in the literature regarding NOx, with most sources affirming an increase while other a decrease, for both the same lipid feedstocks as those used here [28–31] or others [1,34–37]. One reason for this controversy is that NOx emissions are related to the combustion phenomena by chemical factors (i.e. fuel composition in terms of aliphatic chain length and degree of saturation) but also by physical factors (i.e. component parts of the engine as the angle of the spray nozzle of the fuel in the combustion chamber), including type and operating conditions of the diesel engines used [1,2]. As a result, it is difficult to predict NOx emission behavior for a given diesel engine loaded with a given fuel, making experimental tests a prerequisite. Nevertheless, it is admitted that an increase of the ester saturation degree or of the chain length of either of the fatty acid or of the alcohol, leads to a significant NOx reduction. By contrast, an increase of the ignition delay and thus of the temperature inside the combustion chamber even more increased by a higher fuel oxygen content is favorable to NOx emissions [1,2,28–31,34–37].

3.3.2. Particulate matter emissions

PM emissions observed from combustion of all tested fuels are depicted in Table 7 in terms of number concentrations (given

Table 7
Particulate matter emissions (number concentration given globally and per class of average geometric aerodynamic diameter) for petrodiesel B0, the produced biodiesels (BAEEs, AIEEs, JCEEs), and parent NEVO (BA and JC) blended with B0 (mass ratio 50:50).[a]

Fuel	Total number concentration (*10^7, p/cm^3)	PM 0.1 (%)	PM 0.1−1 (%)	PM 1−10 (%)
B0	1.29	32.4	67.4	0.2
BAEEs	1.78	31.3	68.6	0.1
AIEEs	3.56	42.4	57.5	0.1
JCEEs	9.23	32.8	67.0	0.2
[BA:B0]	8.39	48.6	51.2	0.2
[JC:B0]	8.11	47.7	52.0	0.3

[a] PM*x* refers to particulate matter with an average geometric aerodynamic diameter less than *x* microns while PM*x*-*y* refers to the fraction of particles with average geometric aerodynamic diameters comprised between *x* and *y* microns.

globally and per class of average geometric aerodynamic diameter) and in Fig. 6 in terms of number particle size distributions (PSDs). Hence, pollution due to PM emissions could be characterized in terms of environmental effects (with smoke opacity correlated to the PM number concentration) and in terms of human health effects (the smaller particles having the most harmful effects for various reasons: longer residence time in atmosphere, higher specific surface (and thus higher capability to adsorb organic compounds), and higher capability to penetrate into the respiratory and cardio-vascular systems [35]).

It appears clearly that whatever the tested (renewable or fossil) fuel, the PM produced are mainly ultra-fine particles with an average geometric aerodynamic diameter inferior to 1 μm (PM1). In addition, the total number concentration of particles is larger, for all biofuels, than for petrodiesel B0. Among the three classes of FAEEs evaluated, BAEEs showed the best performance with fine PM results (total number concentration and PSD) very close to those obtained with B0, while JCEEs revealed to be the more pollutant fuel in term of total number concentration.

This behavior can be related to the inorganic composition of FAEEs, particularly K and Ca contents (Table 5). It is known that alkaline and alkaline-earth metal oxide are able to catalyze soot oxidation [38−40]. Such a catalytic reaction takes place not only in the exhaust line but also during the soot formation process in the flame since it is observed that, in co-flow flames, the soot particle inception and subsequent coagulation and growth are followed by oxidation [41]. For these three fuels, PSDs are centered on particles with diameter close to 0.2 μm. Nevertheless, the [BA:B0] and [JC:B0] blends have led to even worse behavior by producing, admittedly, lower total particle number concentrations than the JCEE fuel (Table 7), but a PSD shifted towards ultra-fine particles, and then, centered on particles with diameter close to 0.04 μm corresponding to very small particles in the exhaust (Fig. 6). A shift of the PSD towards fine particles (PM0.1−0.3) was also observed with the AIEE fuel (Fig. 6).

As previously discussed for the HC emissions, these results should be related *(i)* to the inferior quality of the JCEEs in terms of ester content and, *(ii)* to the high viscosity of the [NEVO:B0] blends. Regarding the AIEE biodiesel, its high sulfur content due to the parent AI oil combined with a slightly higher viscosity compared to the other ethyl biodiesels (BAEEs and JCEEs) may likely contribute to increase the number of smallest particles (Tables 5−7).

Indeed, higher contents in K and Ca, and also in oxygen in biodiesels because of the ester group in their molecular structure induces reduction in PM emissions by enhanced oxidation, and this all the more efficiently that the ester content in the biodiesel fuel is high. (Tables 4, 5 and 7). In addition, it can be observed that evolution of total number concentration of PM among the three classes of FAEEs is linked with the evolution of HC emissions (Table 7 and A4, Fig. 5). As mentioned previously for the HC emissions, higher viscosity of the fuel makes difficult its atomization/vaporization leading to incomplete combustion and thus, soot formation with production of solid particles and unburned hydrocarbons of low volatility. Hence, observation when using biofuels of a higher total number concentration of particles together with a decrease in their mean diameter supports the assumption of reduction of the solid particle fraction together with an increase of the soluble organic fraction (SOF) as suggested by several authors [35,42], This phenomena is also attributed by the same authors to increased contribution of nucleation mode promoting nanoparticles formation (< 50 nm size) and often associated with hydrocarbon condensation [35,42]. Thus, reduction in solid particle fraction (partly, due to the lack of aromatics in biofuels) would lead to decrease the surface area available for condensation of volatile or semi-volatile organic species. These species together with unburned hydrocarbons of low volatility (all contributing to the SOF) would lead to nanoparticle formation by homogeneous nucleation. This increased contribution of nucleation mode should be all the more significant that viscosity of the considered biofuels is high, explaining the shift of the PSDs towards nanoparticles, particularly observed with the [NEVO:B0] blends. Furthermore, sulfur has often been associated to the formation of the nucleation mode [35], explaining the same trend observed for the AIEE biodiesel and the [NEVO:B0] blends, but for different reasons (sulfur content for the AIEEs and high viscosity for the [NEVO:B0] blends).

Finally, it should be mentioned that PM emissions studied in the literature for methyl biodiesels produced from BA, AI, or JC oils remain subject to controversy, most authors observing reductions while others observed increases in the number of particles with biodiesels [28,30,31]. However, most studies related to FAMEs or FAEEs from various classes of lipid sources have reported decreases in the mean diameter of the PSDs attributed to a sharp decrease in the number of large particles together with increases in the number of the smallest ones [1,9,35,43]. These differences in results obtained in the literature, including the present work, are likely due to the fact that effects of biodiesels on PM emissions are very sensitive to the engine operating conditions. Furthermore, the literature refers most of the time to automotive application and not as the present work to stationary diesel engine [2,9]. Hence, studies of PM emissions by using various classes of biodiesels in power diesel generators should be pursed to prevent any potential negative effect in other context than transportation.

3.3.3. *Carbonyl emissions*

Fig. 7 show carbonyl compound emissions for B0 and the tested biofuels (BAEEs, AIEEs, JCEEs, as well as [BA:B0] and [JC:B0] blends). Numerical results are available in Appendix (Table A5).

Results indicate clearly that with the exception of BAEEs, all tested biofuels (neat AIEEs and JCEEs, or [NEVO:B0] blends) led to an increase of the total carbonyl emissions with respect to B0. The two more pollutant biofuels were the JCEEs and the [JC:B0] blend, with emission levels of +43% and +70% respectively compared to B0. Based on the high concentrations obtained for acrolein

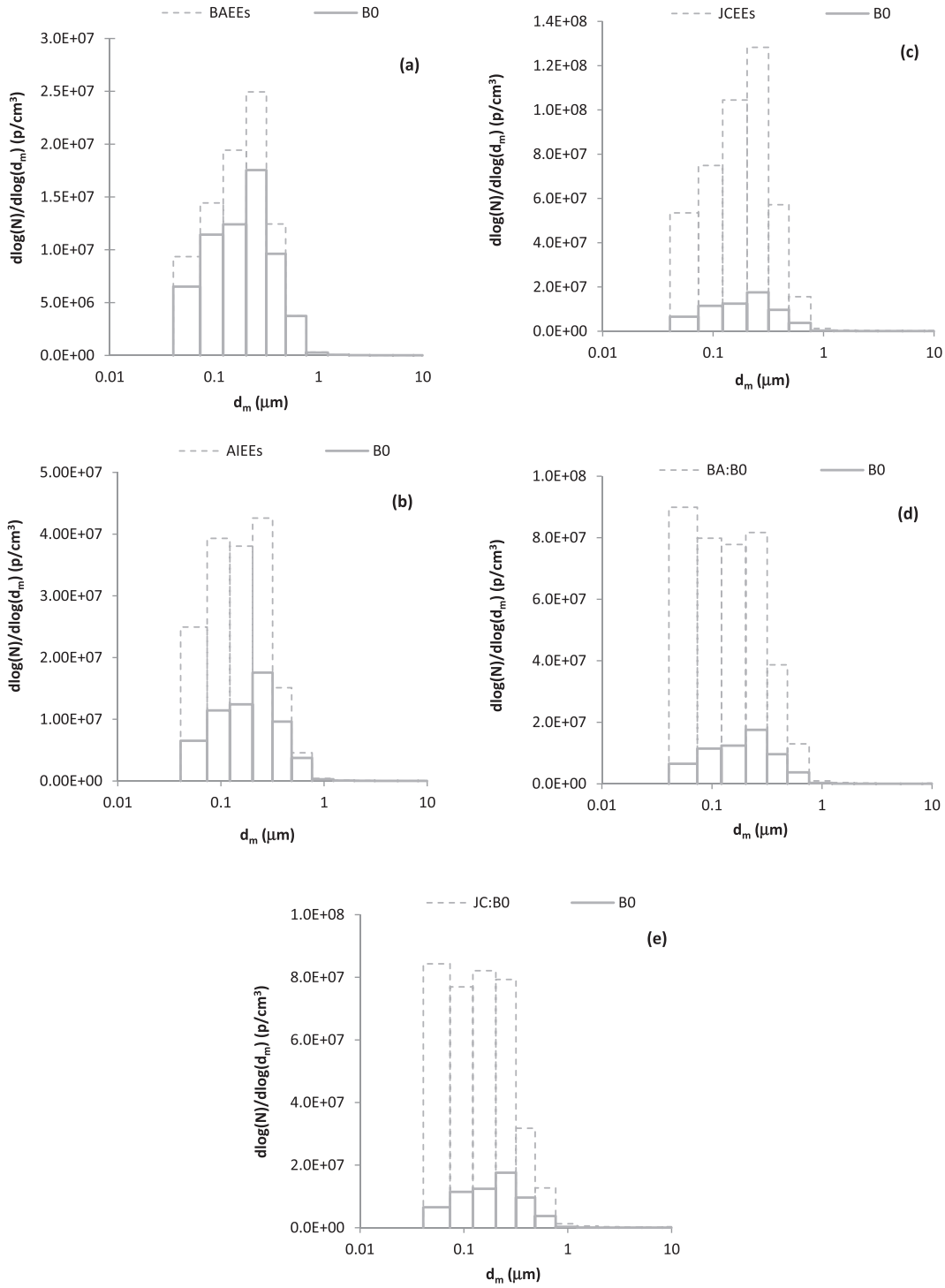

Fig. 6. Fine particle size distributions observed for B0 and the tested biofuels: (a) BAEEs; (b) AIEEs; (c) JCEEs; (d) [BA:B0]; (e) [JC:B0] (mass ratio 50:50 for the NEVO, BA or JC oil, blended with B0).

(gathered with acetone and propanal under the C3 cut, Fig. 7b), this negative behavior is likely due to the high levels in residual free glycerin and glycerides (MG, DG) for the JCEEs, to which should be added the inherent high FFA content of the departure NEVO for the [JC:B0] blend (Table 2) [1,35,42,44].

Moreover, while BAEEs showed lower carbonyl emissions than B0, the [BA:B0] blend revealed to be very hazardous, particularly with regards to formaldehyde and acetaldehyde (which are carcinogenic and mutagenic compounds as well as ozone precursors). As the BAEEs and the parent BA oil have the same composition in fatty acids, the huge difference observed in these harmful emissions should be attributed to the much higher viscosity of BA oil (Table 6), leading to higher production of light aldehydes as products of incomplete combustion [1,9,35,42,44]. Note that this negative impact of the fuel viscosity on formaldehyde emission is also noticeable for [JC:B0] blend with respect to JCEEs.

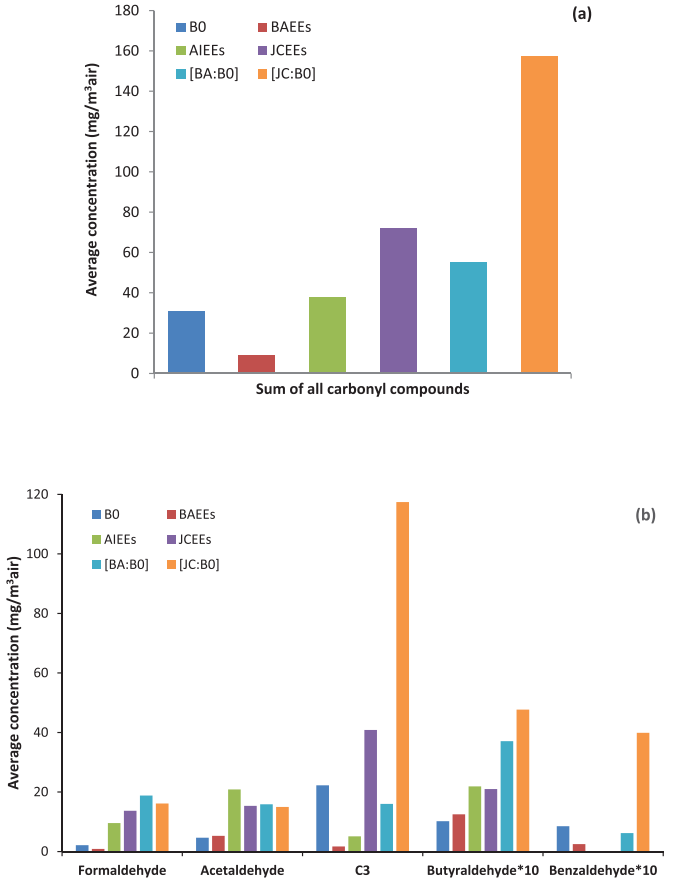

Fig. 7. Carbonyl compound emissions for B0 and the tested biofuels, BAEEs, AIEEs, JCEEs, [BA:B0], [JC:B0] (mass ratio 50:50 for the NEVO, BA or JC oil, blended with B0), (a) by considering carbonyl compounds as a whole, (b) by differentiating the various classes of carbonyl compounds (C3 = Acrolein + Acetone + Propanal).

Regarding the AIEEs, overall they showed almost equivalent performance to B0, with however higher levels of formaldehyde and acetaldehyde (4.5 times), while B0 produced higher levels of acrolein and acetone (6 times, Fig. 7b). The higher content in C16:0 (short saturated fatty acid) of the AIEEs with respect to BAEEs (Table 1) may explain the differences observed in short aldehyde emissions [44].

Similarly to PM emissions, results obtained in this work illustrate the controversy encountered in the literature with respect to carbonyl emissions, with some biofuels showing increases and others some decreases. This highlights the importance of further research on the effects of biodiesel fuel on carbonyl emissions since these may affect human health and environment. Nevertheless, this work helped to show that physical properties of the fuel such as viscosity seem to have a more significant impact on carbonyl emissions than the ester group specific of lipid-based biofuel molecular structure.

4. Conclusions and outlooks

Procedures and operating conditions optimized in laboratory scale for production of FAEEs from widely available NEVOs (BA, AI, and JC oils) [10] were successfully transferred at the pilot scale, with implementation of separation and purification stages.

Although ethanolysis reaction is based on homogeneous catalysis, the proposed alkali route offers a low cost biodiesel production alternative thanks to easy operating conditions (35 °C, atmospheric pressure, ethanol to oil molar ratio of 8, ≈1 wt.% KOH, 50 min), associated with a two-stage procedure based on glycerol recycling and a dry-purification method based on rice husk ashes [8]. Quite satisfactory ester contents were reached for BA and AI-oil derived biodiesels (≈ 91 wt.%). However, further dry-purification cycles should be carried out to make produced biodiesels conformed to commonly admitted specifications (such as EN 14214 standard). Regarding the acid-catalyzed route applied to JC oil with high-FFA content, operating conditions are indeed more severe (78 °C, ethanol to oil molar ratio of 30, 5 wt.% H_2SO_4, 26 h) but make possible hydrated ethanol use (water content: 5 wt.%). By contrast, the dry-purification method of the resulting JCEE product appeared poorly efficient because of the acid nature of the catalyst, leading to a low ester content (84 wt.%). In such circumstance, JC oil pretreatment with crude glycerol recycled from alkali-catalyzed biodiesel production plant should help to carry out FFA neutralization [45] in order to pursue with the proposed low cost alternative.

Exhaust emission analysis via a power generator for the three classes of produced biodiesels (BAEEs, AIEEs, and JCEEs), as well as petrodiesel B0, neat (reference fuel) or blended with crude BA or JC oil (50 wt.%), illustrated the harmful impact of [NEVO:B0] blends and JCEEs, confirming the necessity to convert first the NEVO into biodiesel and this with high FAEE grade for safer use as engine fuel. Quality specifications helped to attribute this hazardous behavior of the [NEVO:B0] blends to the high viscosity of the lipid feedstock, while for JCEEs residual free glycerin and glycerides (MG, DG) were main responsible factors. Regarding AIEEs, desulfurization by organosulfur compound extraction of the parent oil before conversion into biodiesel would be recommended, first to reduce ultrafine PM emission levels and secondly, to recover biologically active species with pharmaceutical interest.

By contrast, BAEEs showed cleaner combustion than petrodiesel. Hence, from the present overall study "feedstock-conversion-engine", a sustainable alternative fuel particularly convenient in rural areas is proposed with BA oil. Agricultural residues from various locally available resources may be used at different stages of the BA-derived bio-refinery: neem or jatropha husks for bioethanol production recycled into ethyl biodiesel synthesis, rice husk ashes for biodiesel dry-purification, upgrading used ashes as natural fertilizers. A further option in agreement with the bio-refinery concept would be to integrate the matter-heat-electricity cogeneration in the biodiesel production unit. This way, the agricultural solid waste combustion would be used to generate heat and power required in the unit operation, while recovering combustion products (ashes) for the purification stage. Consequently, the BAEE alternative described in this work would contribute to a global energy challenge by proposing a sustainable alternative fuel combining [new generation feedstocks - production process - alternative fuel & compatible engine technology] with the constraint of maximizing energy and material efficiency while minimizing environmental and economic impacts [1,2]. Nevertheless, further studies should be conducted by using BAEE as biofuel with different types of engines placed under real operating conditions (actual vehicle for transportation and power generator for the deployment of cogeneration) in order to evaluate the effectiveness of existing pollution control systems.

Acknowledgments

This work has been supported from France by the Communauté Urbaine du Grand Nancy (CUGN), the Conseil Régional d'Aquitaine (20071303002PFM), and the Fonds Européen de Développement Économique et Régional (FEDER) (31486/08011464), and from Burkina Faso by the Fonds National pour l'Education et la Recherche (FONER). Also, the authors would like to express their grateful

acknowledgments to Emilien Girot and Kevin Mozet for their technical support.

Appendix A. Supplementary data

Supplementary data related to this article can be found at http://dx.doi.org/10.1016/j.renene.2017.03.058.

References

[1] L. Coniglio, H. Bennadji, P.A. Glaude, O. Herbinet, F. Billaud, Combustion chemical kinetics of biodiesel and related compounds (methyl and ethyl esters): experiments and modeling Advances and future refinements, Prog. Energy Combust. Sci. 39 (2013) 340–382.

[2] L. Coniglio, J.A.P. Coutinho, J.Y. Clavier, F. Jolibert, J. Jose, I. Mokbel, D. Pillot, M.N. Pons, M. Sergent, V. Tschamber, Biodiesel via supercritical ethanolysis within a global analysis "feedstocks-conversion-engine" for a sustainable fuel alternative, Prog. Energy Combust. Sci. 43 (2014) 1–35.

[3] C. Brunschwig, W. Moussavou, J. Blin, Use of bioethanol for biodiesel production, Prog. Energy Combust. Sci. 38 (2012) 283–301.

[4] M.O.S. Dias, T.L. Junqueira, C.E.V. Rossell, R.M. Filho, A. Bonomi, Evaluation of process configurations for second generation integrated with first generation bioethanol production from sugarcane, Fuel Process. Technol. 109 (2013) 84–89.

[5] H. Haberl, T. Beringer, S.C. Bhattacharya, K.H. Erb, M. Hoogwijk, The global technical potential of bio-energy in 2050 considering sustainability constraints, Curr. Option Environ. Sustain. 2 (2010) 394–403.

[6] I.B. Banković-Ilić, O.S. Stamenković, V.B. Veljković, Biodiesel production from non-edible plant oils, Renew. Sustain. Energy Rev. 16 (2012) 3621–3647.

[7] A. Karmakar, S. Karmakar, S. Mukherjee, Biodiesel production from neem towards feedstock diversification: Indian perspective, Renew. Sustain. Energy Rev. 16 (2012) 1050–1060.

[8] S. Nitièma-Yefanova, R. Richard, S. Thiebaud-Roux, B. Bouyssiere, Y.L. Bonzi-Coulibaly, R.H. Nébié, K. Mozet, L. Coniglio, Dry-purification by natural adsorbents of ethyl biodiesels derived from nonedible oils, Energy Fuels 29 (2015) 150–159.

[9] A.-F. Cosseron, H. Bennadji, G. Leyssens, L. Coniglio, T.J. Daou, V. Tschamber, Evaluation and treatment of carbonyl compounds and fine particles emitted by combustion of biodiesels in a generator, Energy & Fuels 26 (2012) 6160–6167.

[10] S. Nitièma-Yefanova, L. Coniglio, R. Schneider, R.H.C. Nébié, Y.L. Bonzi-Coulibaly, Ethyl biodiesel production from non-edible oils of *Balanites aegyptiaca, Azadirachta indica*, and *Jatropha curcas* seeds – laboratory scale development, Renew. Energy 96 (2016) 881–890.

[11] S. Nitièma-Yefanova, G. Son, S. Yé, R.H.C. Nébié, Y. Bonzi-Coulibaly, Optimisation des paramètres d'extraction à froid de l'huile d'*Azadirachta indica* A. Juss et effets sur quelques caractéristiques chimiques de l'huile extraite, Biotechnol. Agron. Soc. Environ. 16 (2012) 423–428.

[12] S. Nitièma-Yefanova, J.H. Poupaert, E. Mignolet, R.C.H. Nébié, L.Y. Bonzi-Coulibaly, Characterization of some nonconventional oils from Burkina Faso, J. Soc. Ouest Afr. Chim. 033 (2012) 67–71.

[13] EN-14104, Fat and Oil Derivatives, Fatty Acid Methyl Esters (FAME), Determination of Acid Value, European Committee for Standardization, Brussels (Belgium), 2003.

[18] C. Namasivayam, D. Sangeetha, R. Gunasekaran, Removal of anions, heavy metals, organics and dyes from water by adsorption onto a new activated Carbon from Jatropha husk, an agro-industrial solid waste, Process Saf. Environ. Prot. 85 (2007) 181–184.

[19] C. Cossart, Transesterification of Waste Cooking Oil (WCO) Using Alkali Catalyst and Emissions of Fatty Acid Ethyl Esters (FAEEs) during Combustion, Master's Thesis, Université de Lorraine, France, 2010.

[20] W. Zhou, D.G.B. Boocock, Phase distributions of alcohol, glycerol, and catalyst in the transesterification of soybean oil, J. Am. Oil Chem. Soc. 83 (2006) 1041–1045.

[21] A.-F. Cosseron, V. Tschamber, L. Coniglio, T.J. Daou, Study of Non-Regulated Exhaust Emissions Using Biodiesels and Impact on a 4 Way Catalyst Efficiency, SAE International Meeting, Technical Paper N° 2011-24-0194, doi:10.4271/2011-24-0194.

[22] EN-14103, Fat and Oil Derivatives, Fatty Acid Methyl Esters (FAME), Determination of Ester and Linoleic Acid Methyl Ester Contents, European Committee for Standardization, Brussels (Belgium), 2003.

[23] M. Berrios, M.A. Martín, A.F. Chica, A. Martín, Purification of biodiesel from used cooking oils, Appl. Energy 88 (2011) 3625–3631.

[24] A.E. Atabani, A.S. Silitonga, I.A. Badruddin, T.M.I. Mahlia, H.H. Masjuki, S. Mekhilef, A comprehensive review on biodiesel as an alternative energy resource and its characteristics, Renew. Sustain. Energy Rev. 16 (2012) 2070–2093.

[25] M.F. Balandrin, S.M. Lee, J.A. Klocke, Biologically active volatile organosulfur compounds from seeds of the Neem tree, *Azadirachta indica (Meliaceae)*, J. Agric. Food Chem. 36 (1988) 1048–1054.

[26] A.M. Mubarak, C.P. Kulatilleke, Sulphur constituents of Neem seed volatiles: a revision, Phytochemistry 29 (1990) 3351–3352.

[27] O.S. Valente, M.J. da Silva, V.M.D. Pasa, C.R.P. Belchior, J.R. Sodré, Fuel consumption and emissions from a diesel power generator fuelled with castor oil and soybean biodiesel, Fuel 89 (2010) 3637–3642.

[28] M. Mofijur, M.G. Rasul, J. Hyde, A.K. Azad, R. Mamat, M.M.K. Bhuiya, Role of biofuel and their binary (diesel–biodiesel) and ternary (ethanol–biodiesel–diesel) blends on internal combustion engines emission reduction, Renew. Sustain. Energy Rev. 53 (2016) 265–278.

[29] S.J. Deshmukh, L.B. Bhuyar, Transesterified Hingan (Balanites) oil as a fuel for compression ignition engines, Biomass Bioenergy 33 (2009) 108–112.

[30] M. Takase, T. Zhao, M. Zhang, Y. Chen, H. Liu, L. Yang, X. Wu, An expatiate review of neem, jatropha, rubber and karanja as multipurpose non-edible biodiesel resources and comparison of their fuel, engine and emission properties, Renew. Sustain. Energy Rev. 43 (2015) 495–520.

[31] M. Habibullah, H.H. Masjuki, M.A. Kalam, S.M. Ashrafur Rahman, M. Mofijur, H.M. Mobarak, A.M. Ashraful, Potential of biodiesel as a renewable energy source in Bangladesh, Renew. Sustain. Energy Rev. 50 (2015) 819–834.

[32] L.F. Ramírez-Verduzco, J.E. Rodríguez-Rodríguez, A.R. Jaramillo-Jacob, Predicting cetane number, kinematic viscosity, density and higher heating value of biodiesel from its fatty acid methyl ester composition, Fuel 91 (2012) 102–111.

[33] K. Sivaramakrishnan, P. Ravikumar, Determination of cetane number of biodiesel and its influence on physical properties, ARPN J. Eng. Appl. Sci. 7 (2012) 205–211.

[34] R.L. McCormick, M.S. Graboski, T.L. Alleman, A.M. Herring, K.S. Tyson, Impact of biodiesel source material and chemical structure of emissions of criteria pollutants from heavy duty engines, Environ. Sci. Technol. 35 (2001) 1742–1747.

[35] M. Lapuerta, O. Armas, J. Rodriguez-Fernandez, Effect of biodiesel fuels on diesel engine emissions, Prog. Energy Combust. Sci. 34 (2008) 198–223.

[36] K. Kohse-Höinghaus, P. Oβwald, T.A. Cool, T. Kasper, N. Hansen, F. Qi, C.K. Westbrook, P.R. Westmoreland, Biofuel combustion chemistry: from ethanol to biodiesel, Angew. Chem. Int. Ed. 49 (2010) 3572–3597.

[37] M.J. Abedin, M.A. Kalam, H.H. Masjuki, M.F.M. Sabri, S.M. Ashrafur Rahman, A. Sanjid, I.M. Rizwanul Fattah, Production of biodiesel from a non-edible source and study of its combustion, and emission characteristics: a comparative study with B5, Renew. Energy 88 (2016) 20–29.

[38] K. Tikhomirov, O. Kröcher, A. Wokaun, Influence of potassium doping on the activity and the sulfur poisoning resistance of soot oxidation catalysts, Catal. Lett. 109 (2006) 49–53.

[39] R. Jiménez, X. García, C. Cellier, P. Ruiz, A.L. Gordon, Soot combustion with K/MgO as catalyst, Appl. Catal. A General 297 (2006) 125–134.

[40] L. Castoldi, R. Matarrese, L. Lietti, P. Forzatti, Intrinsic reactivity of alkaline and alkaline-earth metal oxide catalysts for oxidation of soot, Appl. Catal. B Environ. 90 (2009) 278–285.

[41] K.T. Kang, J.Y. Hwang, S.H. Chung, W. Lee, Soot zone structure and sooting limit in diffusion flames: comparison of counter-flow and co-flow flames, Combust. Flame 109 (1997) 266–281.

[42] G. Fontaras, G. Karavalakis, M. Kousoulidou, T. Tzamkiozis, L. Ntziachristos, E. Bakeas, S. Stournas, Z. Samaras, Effects of biodiesel on passenger car fuel consumption, regulated and non-regulated pollutant emissions over legislated and real-world driving cycles, Fuel 88 (2009) 1608–1617.

[43] G. Fontaras, G. Karavalakis, M. Kousoulidou, L. Ntziachristos, E. Bakeas, S. Stournas, Z. Samaras, Effects of low concentration biodiesel blend application on modern passenger cars. Part 1: feedstock impact on regulated pollutants, fuel consumption and particle emissions, Environ. Pollut. 158 (2010) 1451–1460.

[44] G. Fontaras, G. Karavalakis, M. Kousoulidou, L. Ntziachristos, E. Bakeas, S. Stournas, Z. Samaras, Effects of low concentration biodiesel blends application on modern passenger cars. Part 2: impact on carbonyl compound emissions, Environ. Pollut. 158 (2010) 2496–2503.

[45] L.L. Sousa, I.L. Lucena, F.A.N. Fernandes, Transesterification of castor oil: effect of the acid value and neutralization of the oil with glycerol, Fuel Process. Technol. 91 (2010) 194–196.